A NEW FEM APPROACH TO PREDICT RESIDUAL STRESS PROFILES IN HARD TURNING WITHOUT SIMULATING CHIP FORMATION

S. Anurag, Y.B. Guo
Dept. of Mechanical Engineering
The University of Alabama, Tuscaloosa, AL 35487, USA

Z.Q. Liu
School of Mechanical Engineering
Shandong University, Jinan, 250061, PR China

KEYWORDS

Residual stress profile, plowed depth, size effect, finite element modeling, hard turning.

ABSTRACT

Residual stress prediction in hard turning has been recognized as one of the most important and challenging tasks. A hybrid finite element predictive model has been developed with the concept of plowed depth to predict residual stress profiles in hard turning. With the thermo-mechanical work material properties, residual stress has been predicted by simulating the dynamic turning process followed by a quasi-static stress relaxation process. The residual stress profiles were predicted for a series of plowed depths potentially encountered in machining. The predicted residual stress profiles agree with the experimental one in general. A transition of residual stress profile has been recovered at the critical plowed depth. In addition, the effects of cutting speed, friction coefficient and inelastic heat coefficient on residual stress profiles have also been studied and explained.

INTRODUCTION

Hard turning and grinding are the major finish machining processes. Apart from process efficiency, flexibility and cost, residual stress is a major concern since it significantly affects the performance of machined components subjected to dynamic loading and aggressive environments. In machining, residual stress is determined by the deformation state which is characterized by strain, strain rate, temperature, and complex loading/coupling histories and microstructural evolution.

Generally speaking, the magnitude and pattern of a resultant stress profile is determined by physical and mechanical properties of the work material as well as machining parameters. In hard turning, two major factors are responsible for the resulted residual stress. First, cutting force induces local plastic deformation which tends to induce compressive residual stresses in the subsurface. Second, high temperatures resulted from the plastic deformation and tool/workpiece friction may cause tensile residual stress and phase transformations such as white layer in the subsurface. Tensile residual stress and white layer are detrimental to the service life of machined parts because they promote crack formation and failure progression.

Residual stress measurement by X-ray diffraction and other methods are time consuming and expensive. An accurate simulation approach to predict residual stress profile can facilitate design and optimize a hard turning process. Since finite element analysis (FEA) is capable of incorporating the process physics in a model, it is inarguably one of the most powerful and reliable tools at present for accurate prediction of residual stress profiles.

LITERATURE REVIEW

Several researchers [Matsumoto et al., 1986, 1999; Warren and Guo, 2009] investigated the nature of residual stress by hard truning employing various measurement techniques. It's found that residual stress profiles display distinct patterns in the subsurface for turning and grinding operations. Hard turning using a sharp tool usually generates a maximum compressive stress in the subsurface while grinding leaves maximum compressive residual stress at the surface. The nature of machining induced residual stress profiles was also reported by other researchers [Brinksmeier et al., 1982; Thiele and Melkote, 2000; Dahlman et al., 2004]. They showed that machining parameters like depth of cut, feed, cutting speed, tool geometry have its individual contribution to residual stress magnitude instead of profile pattern. These significant observations drove research focus in the prediction of residual stress profile patterns, yet the work in this direction is still in its infancy. It implies that a successful prediction of residual stress must recover these distinct profiles.

Sasahara et al. [1996] and Liu and Guo [2000] utilized FEA models to simulate the variation of residual stress profile in sequential cutting. The experimental and simulation confirmed that compressive residual stress can be generated by fine cutting following a rough cutting. Liu and Guo [2000] further showed that residual stress prediction is sensitive to friction condition between tool/workpiece. Following this proposition, Guo and Liu [2002] developed a practical explicit 3D finite element method (FEM) model to analyze turning AISI 52100 hardened steel using a polycrystalline cubic boron nitride (PCBN) cutting tool. The influence of edge geometry in 3D turning simulation on process variables are also reported [Ozel, 2009]. Sasahara et al [2004] proposed a process model for the prediction of surface residual stress caused by machining by combining an FEA orthogonal cutting simulation with a tool corner's indentation model. The process model could predict residual stress becoming compressive with small corner radius tool and it changes from tension to compression as feed rate decreases. Analytical models have also been developed to predict residual stresses in a turning process [Jacobus et al., 2001].

The thermoelastic-plastic properties of the workpiece material have been incorporated in most FEA machining simulations. Although a certain success has been achieved in predicting residual stress, the complex modeling and time-consuming calculations impose a great concern on its practical applications. Most FEA prediction models suffer from sufficient accuracy in terms of residual stress profile pattern due to the assumptions and simplifications of a physical process. The neural network approach has a major disadvantage that it needs a huge amount of experiment data for input. Therefore, a practical physical FEA model for residual stress prediction in machining is still lacking.

A practical FEA model should be able to simulate the cutting process (step1) followed by a stress relaxation process (step 2) in order to predict residual stress. However, few researches have conducted the two-step simulations. A cutting process is a large deformation process involving severe element distortions which dumps a simulation before the tool cuts through a workpiece. It is imperative that a machining simulation for predicting residual stress has to be carried out with sufficient cutting length to avoid any edge effects. In addition, the instances of frequent element distortions cause abrupt fluctuations in surface deformation and thus it is difficult to generate a consistent residual stress profile along the subsurface depth. Therefore, the objectives are to:

- Create a hybrid FEA method with the concept of plowed depth to predict residual stress profiles by incorporating both cutting and forming features around cutting edge.
- Conduct a two-step simulation with sufficient cutting length for reliable predictions.
- Provide a new physical insight on how the plowed depth affects the evolution of residual stress profile patterns.
- Study the sensitivity of residual stress profile to cutting speed, friction, and the heat conversion factor of plastic deformation.

SIMULATION SCHEME

Concept of plowed depth

In machining, when the tool advances in the workpiece in cutting direction to form the chip, it exerts tremendous pressure on work material in cutting direction as well as a significant amount of thrust in the downward direction. The cutting force causes partial work material to separate in the form of a chip over the tool's rake face.

However, the thrust force causes the material to flow under the tool's cutting edge radius. The phenomenon of material flowing under the cutting edge is termed as plowing in the literature. The point where the material flow separates to form the chip and machined surface is known as stagnation point [Guo and Wen, 2005]. The material plowed under the tool experiences severe plastic deformation and high temperatures, and forms the top layer of the machined surface. The resulting surface integrity of the workpiece is determined by the deformation state of this thin plowed layer. The amount of material plowed under the cutting edge largely depends on the cutting edge geometry. The stress state and temperatures during cutting and residual stress after cutting are significantly determined by the amount of plowed material. Therefore, the plowed depth is assumed to be the most important factor to shape residual stress profile, while chip formation region would have little contribution (about 10-20%).

In order to illustrate the hybrid approach, a schematic relationship between stagnation point and cutting edge is presented in Fig. 1. Point O is the center of cutting edge, point A is the position where the chip leaves the tool rake face, and point B is the location where the machined surface separates from the tool flank face. Point P is the stagnation point and PC is the actual material separation line, while BD is the ideal separation line. The actual uncut chip thickness and the ideal uncut chip thickness are t_1 and t_2, respectively. The tool edge radius is r and chamfer angle is θ. The stagnation angle is α. VB represents tool flank wear which is not incorporated in the present work. The plowed depth δ can be expressed as

$$\delta = t_2 - t_1 = r\,(1 - \cos\alpha) \quad (1)$$

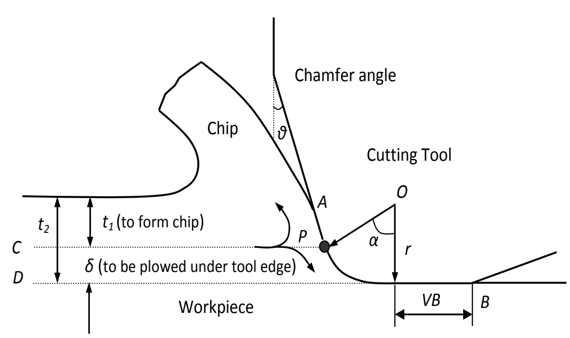

FIG. 1 PLOWED DEPTH IN CUTTING.

A δ value represents the amount of material that gets plowed under the cutting edge to form the machined surface. According to Eq. 1, if the stagnation angle α is known, the plowed material amount δ can be determined given the edge radius r. For most materials and cutting conditions, stagnation angle varies within a certain range [Guo and Wen, 2005].

According to the hypothesis, the chip formation zone (above line PC) would have little contribution to residual stress and therefore was not modeled. Only the plowed depth (below line PC) was modeled and simulated. Therefore the workpiece mesh is designed for plowing process where the plowed depth δ is defined by the stagnation angle α. For continuous plowing along the workpiece length and to eliminate the possible severe element distortions in the plowed depth, adaptive mesh was utilized in the model to facilitate the nodes and elements to adjust themselves with the deformation without affecting the accuracy of the numerical simulations.

Simulation conditions

For the comparative study of effect of plowed depth on resulting residual stress in the machining simulation, five values of α in the range of 20º - 50º were used. It corresponds to five levels of plowed depth δ in Table 1. Plane strain element type CPE4RT of 4-node and reduced integration elements with temperature degrees of freedom was used to mesh the workpiece, Fig. 2. To reduce computation time as well as ensuring a sufficient cutting distance and eliminate possible size effect and edge effect, the overall workpiece dimensions are 500 μm × 100 μm. The workpiece top was meshed with fine elements of size 1 μm × 1 μm whereas the bottom was meshed with a relatively coarse mesh. The workpiece bottom was modeled using semi-infinite elements as quiet boundary. The rigid tool with 6 clearance angle was constrained to move in cutting direction only and the initial temperature of workpiece was set to 293K. The adiabatic condition was imposed with inelastic heat coefficient 0.9 and tool/work friction coefficient as 0.1 due to the low friction capability of the PCBN cutting tool.

TABLE 1 CUTTING SIMULATION CONDITIONS.

r (μm)	α (º)	δ (μm)	V (m/s)	θ (º)
10	30	1.3	2.5	15
10	35	1.8	2.5	15
10	40	2.3	2.5	15
10	45	2.9	2.5	15
10	50	3.6	2.5	15

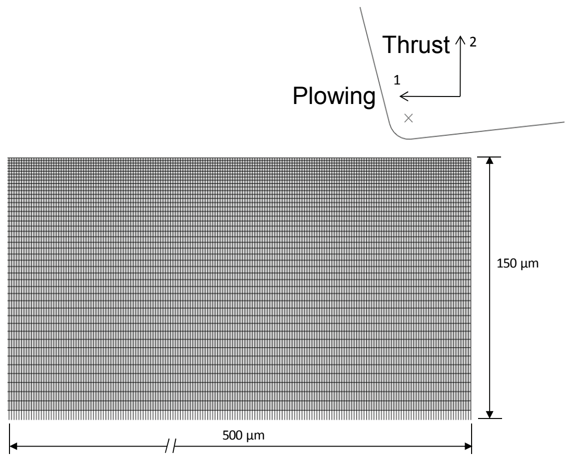

FIG. 2 SETUP OF CUTTING SIMULATION.

Two-step simulation procedures

Material modeling. The dynamic mechanical behavior of AISI 52100 bearing steel was modeled using the internal state variable plasticity model [Bammann et al., 1996]. The material constants were obtained from a series of material tests and curve fitting [Guo et al., 2006] over a wide range of strains and temperatures. The material constants were incorporated into Abaqus/Explicit [HKS, 2008] via the user subroutine VUMAT where all the constitutive equations of the model were coded. Table 2 lists the material constants of 52100 steel used for the simulations.

Plowing process simulation. In the plowing process simulation, after attaining the defined plowed depth δ the tool moves in cutting direction and starts to plow the material ahead of it. The chipless plowing process should result in reasonable stress, strain and temperature fields and significantly reduced computation time. The plowing process is similar to burnishing [Sartkulvanich et al., 2007]. However, the tool/work contact mechanics or nature is fundamentally different due to the realistic cutting tool geometry and plowed depth.

The mechanical state of the workpiece after tool cutting sliding over the workpiece contains transient stresses, strains, and temperatures due to plowing. For residual stress prediction, the transient state needs to be relaxed by cooling the workpiece to room temperature.

Relaxation simulation. Residual stress analysis is a static process and therefore the Abaqus/Standard module is utilized. In order to arrive at realistic results, it is important to import the true mechanical state from the last step of previous plowing simulation by Abaqus/Explicit. Therefore, the workpiece mesh was imported in Abaqus/Standard with stresses and temperatures at all elements and nodes. Using the thermal properties of bearing steel, each case was submitted for static analysis in a fully coupled thermomechanical simulation. The stress analysis initially results in the dissipation of workpiece temperature to a uniform value in the due course of time. Thereafter the whole workpiece cools down to room temperature and thus stress relaxation was achieved.

TABLE 2 BCJ MATERIAL CONSTANTS OF AISI 52100 (62 HRC) FOR USER SUBROUTINE VUMAT.

Material constants	Tension mode
Shear Modulus G_0 (Pa)	7.85E+10
a	1.23E+00
Bulk Modulus K_0 (Pa)	1.52E+11
b	-1.85E+10
Melting point(K)	1.64E+03
C_1 (MPa)	1.00E+00
C_2 (K)	1.00E+00
C_3 (MPa)	1.07E+03
C_4 (K)	1.00E+00
C_5 (1/s)	1.00E+00
C_6 (K)	-1.20E+04
C_7 (1/MPa)	4.00E-02
C_8 (K)	0.00E+00
C_9 (MPa)	5.60E+03
C_{10} (MPa/K)	2.00E+01
C_{11} (s/MPa)	2.385E-03
C_{12} (K)	4.00E+02
C_{13} (1/MPa)	5.50E-01
C_{14} (K)	3.00E+02
C_{15} (MPa)	6.00E+05
C_{16} (MPa/K)	5.36E+02
C_{17} (s/MPa)	3.50E-04
C_{18} (K)	4.00E+03
C_{19}	1.00E-01
C_{20} (K)	6.73E+02
C_{21}	0.00E+00
Initial temperature (K)	2.93E+02
Heat Coefficient (m^3K/J)	2.43E-07
Initial damage	0.01E+00
Damage exponent	3.00E+00

In the plowing simulation, the maximum temperature was recorded immediately under the cutting tool whereas in residual stress simulation, the residual stress was recorded from middle of the workpiece by eliminating size effect. Fig. 3 shows the path to retrieve temperature profile in plowing and residual stress profile after cooling.

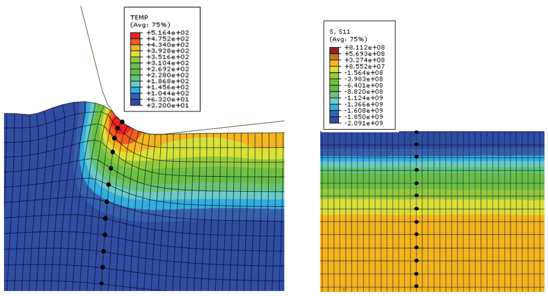

FIG. 3 NODE PATH TO RETRIEVE TEMPERATURE AND RESIDUAL STRESS PROFILES.

RESULTS AND DISCUSSION

Plowing force

The reaction force components, Fig. 4, in cutting and thrust directions at each plowed depth are individually retrieved during the entire plowing period. As expected a certain fluctuation of both forces is also shown by the average and variations as the tool slides over the surface.

As seen in Fig. 4a, the plowing force increases with the increased plowed depth. However, a sharp increase of plowing force occurs when the plowed depth increases from 0.6 μm to 1.3 μm, then the increase rate significantly decreases with the plowed depth. In contrast, the thrust force in Fig. 4b behaves very differently. The thrust force initially increases when the plowed depth increases from 0.6 μm to 1.3 μm, then becomes relatively stable at larger plowed depths. However, the magnitudes of thrust force are much larger than the corresponding plowing force. In other words, the thrust/plowing force ratio decreases significantly from low plowed depth to the large ones.

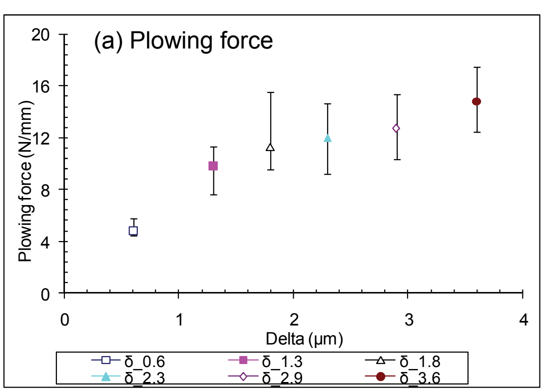

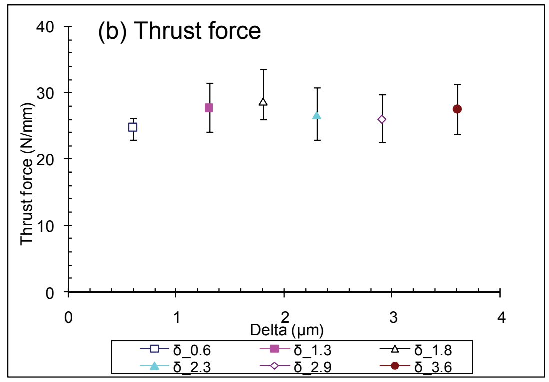

FIG. 4 FORCE VARIATION WITH THE PLOUGHED DEPTH.

Residual stress evolution

Fig. 5a shows the predicted residual stress profiles in cutting direction after the workpiece cooled to room temperature. At small plowed depth of 1.3 μm and 1.8 μm, the residual stress profile shows that the maximum compressive residual stress at the surface and decreases rapidly towards the tensile region within a shallow near-surface of 14 μm. The predicted patterns of residual stress profiles closely match those measured data of ground surfaces in the literature [Warren and Guo, 2009]. At larger plowed depths of 2.3 μm, 2.9 μm, and 3.6 μm, the magnitudes of predicted compressive residual stresses are significantly reduced at the surface. However, the maximum compressive residual stresses occur at 8 μm - 12 μm in the subsurface. The predicted "hook" shaped residual stress profiles resemble the characteristics of measured residual profiles of turned surfaces with sharp tools.

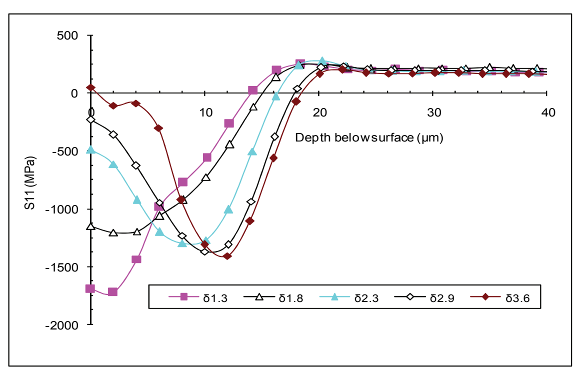

FIG. 5A RESIDUAL STRESS S11 PROFILE (μ=0.1, h=0.9).

The following two observations regarding the affected subsurface region are noteworthy here.

First, the zone of predicted compressive residual stress at the large plowed depths is much larger (20 μm vs. 14 μm) than that at small plowed depths. Second, the predicted compressive residual stresses at the surface for small plowed depths are much larger than those at the larger plowed depths. Therefore, it can be inferred that for smaller plowed depths, the deformation energy dissipates at the surface with high magnitude affecting a shallow near-surface, whereas, for larger plowed depths, the energy dissipates somewhere deeper in subsurface with lower magnitude and affecting a larger depth.

The predicted residual stress profile at the plowed depth of 1.8 μm seems to serve as a transition case from a grinding dominated process to a turning dominated process. The comparison indicates that the a large plowed depth will predict characteristic residual stress profiles of turning with sharp tools, while a small plowed depth will predict residual stress profiles of grinding with sharp wheels. This is because a small δ value corresponds to the process conditions of grinding in terms of shallow depth of cut, whereas the large δ value represents turning conditions employing a large depth of cut. In other words, material plowed under the cutting edge is more in hard turning than in grinding. Therefore, the plowed depth is the most important controlling factor for residual stress profiles in hard turning as well as grinding.

Fig. 5b shows the predicted temperature profiles in the subsurface recorded under the cutting edge during plowing simulation. It can be seen that temperature increases with the plowed depth. A larger δ value implies more plowing of the material. More material deformation is converted to thermal energy during simulations. Since the maximum surface temperature 515°C at the largest plowed depth is well below the phase transformation temperature (~723°C) of AISI 52100 steel, it justifies the simulation assumption that no phase transformation occurs in the workpiece. However, in case of tool flank wear, higher temperatures are expected to result in phase transformations.

Residual stress sensitivity to cutting speed

To investigate residual stress sensitivity to cutting speed all the simulation cases in Table 1 were re-simulated with tool velocity changed from 2.5 m/s to 25 m/s. It has been observed that the simulations of only two cases with small δ values are successful. This is because such a high velocity is not feasible for high δ values which typically represent hard turning conditions with large depth of cut. To understand how high velocity affects the overall material's thermomehanical deformation, residual stress was plotted in Fig. 6. Residual stress at the surface shifted from high compressive to tensile due to the increased temperature at high cutting speeds. The larger the plowed depth, the larger influence of cutting speed on residual stress.

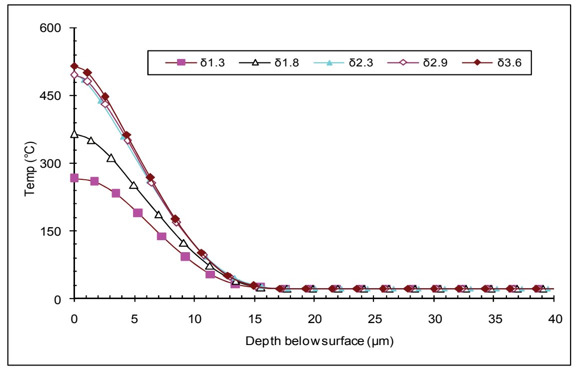

FIG. 5B TEMPERATURE PROFILE UNDER CUTTING EDGE (μ=0.1, h=0.9).

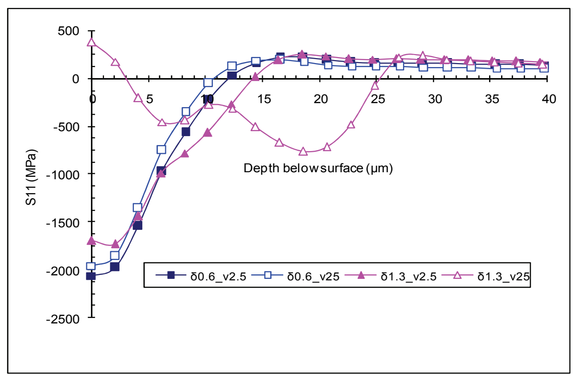

FIG. 6 RESIDUAL STRESS SENSITIVITY TO CUTTING VELOCITY (μ=0.1, h=0.9).

Residual stress sensitivity to friction

The effect of increased tool/work friction on residual stress profiles is shown in Fig. 7 with the friction coefficient 0.1 and 0.3. Surface residual stresses shifts toward to tensile region due to the expected increase of temperatures, while the basic characteristics of hooked shaped profiles remain unchanged. The friction coefficient effect on residual stress is larger for the small plowed depth than the large ones.

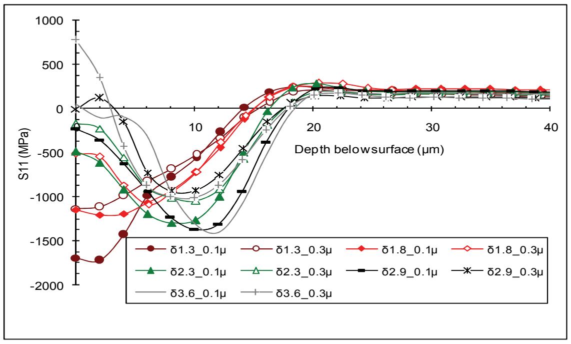

FIG. 7 RESIDUAL STRESS SENSITIVITY TO FRICTION COEFFICIENT (v=2.5m/s, h=0.9).

Residual stress sensitivity to inelastic heat coefficient

The inelastic heat coefficient represents how much plastic deformation can be converted to thermal energy. In metal cutting process, the coefficient is usually 90%. However, 100% could happen at high cutting speeds such as hard turning. Therefore, the sensitivity of residual stress profiles to the inelastic heat coefficient was investigated by increasing the value from 0.9 to 1.0. Fig. 8 shows residual stress profiles for all the simulation cases. The magnitudes of compressive residual stress at the surface also slightly decrease due to the slightly increased temperature. However, the hook shaped residual stress profile pattern remains unaltered.

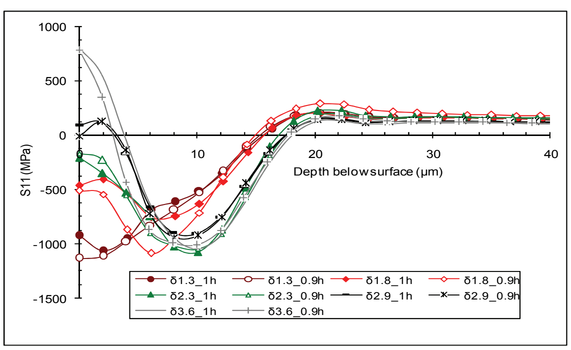

FIG. 8 RESIDUAL STRESS SENSITIVITY TO INELASTIC HEAT COEFFICIENT (v=2.5m/s, μ=0.3).

EXPERIMENTAL ANALYSIS

To further verify the predicted characteristics of residual stress profiles by hard turning and grinding, face turning AISI 52100 steel (62 HRc) discs of 76.2 mm diameter and 19.05 mm thickness was conducted on a rigid, high precision lathe with a GE BZN 8100 round tool (0.15mm/15º chamfer & 6.35 mm tool radius). Surface grinding was also conducted on the same work material with a fresh aluminum grinding wheel with water soluble coolant. Fig. 9 shows that measured residual stress profiles with variations by the X-ray diffraction method.

Several differences in residual stress profiles by hard turning and grinding were observed. In the feed direction, the maximum compressive residual stress occurs on the surface for the case of grinding while it is located in the subsurface for hard turning. The magnitude and affected depth of compressive residual stress are greater for hard turning. Due to the gentle machining conditions used for both surfaces types, the affected depth of residual stress is rather shallow (<20 μm). In the cutting (or grinding) direction there is also a noticeable difference. For both hard turning and grinding, the maximum compressive residual stress occurs on the surface. While residual stress on the turned surface has a relatively large variation. It implies that a "hook" shaped residual stress profile still may occur in the cutting direction. In addition, the magnitude of residual stress generated by hard turning is more than 3 times larger than that for grinding and the affected depth is nearly twice as deep. The observed differences in residual stress profiles can also be seen in the predicted ones in Fig. 5a. It should be pointed out that the predicted patterns of residual stress profiles instead of magnitudes were compared to the test data since an identical orthogonal cutting and simulation condition is very difficult to achieve.

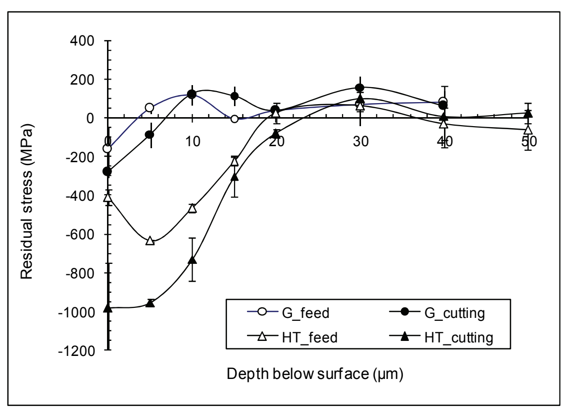

FIG. 9 MEASURED RESIDUAL STRESS PROFILES (AVERAGE, MAX, AND MIN) FROM EXPERIMENTS.

CONCLUSIONS

A coupled thermal-mechanical based hybrid FEA modeling approach without explicit chip formation has been developed to predict characteristics of residual stress profiles by hard turning. Key findings are summarized as follows.

- The ploughed depth is the single most important controlling factor for the unique characteristics of residual stress profiles.
- The predicted characteristics of residual stress profiles favorably agree with the measured ones.
- The increased cutting speed and tool/work friction, and inelastic heat coefficient reduce the magnitudes of compressive residual stress at the surface, but the hook shaped residual stress profile pattern remains unaltered.

ACKNOWLEDGEMENT

This research is based upon the work supported by the NSF CMMI-0447452 and NSFC-50828501.

REFERENCES

Bammann D.J., M.L. Chiesa and G.C. Johnson (1996). “Modeling large deformation and failure in manufacturing processes.” *Theo. App. Mech.*, 359–376.

Brinksmeier E., J.T. Cammett, W. Koenig, P. Leskovar, J. Peters and H.K. Toenshoff (1982). “Residual stresses measurement and causes in machining processes.” Ann. CIRP, 31, 491-510.

Dahlman P., F. Gunnberg and M. Jacobson (2004). “The influence of rake angle, cutting feed and cutting depth on residual stresses in hard turning.” J. Mater. Proc. Tech., 147, 181-184.

Guo Y.B. and C.R. Liu (2002). “3D FEA modeling of hard turning.” J. Manuf. Sci. Eng., 124, 198–199.

Guo Y.B. and Q. Wen (2005). “A hybrid modeling approach to investigate chip morphology transition with the stagnation effect by cutting edge geometry.” Trans. SME/NAMRI, 33, 469-476.

Guo Y.B., Q. Wen and K.A. Woodbury (2006). “Dynamic material behavior modeling using internal state variable plasticity and its application in hard machining simulations.” J. Manuf. Sci. Eng., 128, 749-759.

HKS Inc, 2008, *ABAQUS Manual*, v6.8.

Jacobus K., R.E. DeVor, S.G. Kapoor and R.A. Peascoe (2001). “Predictive model for the full biaxial surface and subsurface residual stress profiles from turning.” J. Manuf. Sci. Eng., 123, 537-546.

Liu C.R. and Y.B. Guo (2000). “Finite element analysis of the effect of sequential cuts and tool–chip friction on residual stresses in a machined layer.” Int. J. Mech. Sci., 42, 1069-1086.

Matsumoto Y., M.M. Barash and C.R. Liu (1986). “Effect of hardness on the surface integrity of AISI 4340 steel”, J. Eng. Ind., 180, 169-175.

Matsumoto Y., F. Hashimoto and G. Lahoti (1999). “Surface integrity generated by precision hard turning.” Ann. CIRP, 48/1, 59-62.

Ozel T. (2009). “Computational modelling of 3D turning: Influence of edge micro-geometry on forces, stresses, friction and tool wear in PCBN tooling.” J. Mater. Proc. Tech., 209, 5167-5177.

Sartkulvanich P., T. Altan, F. Jasso and C. Rodriguez (2007). “Finite element modeling of hard roller burnishing: an analysis on the effects of process parameters upon surface finish and residual stresses.” J. Manuf. Sci. Eng., 129, 705-716.

Sasaharaa H., T. Obikawa and T. Shirakashi, (1996). “FEM analysis of cutting sequence effect on mechanical characteristics in machined layer.” J. Mater. Proc. Tech., 62, 448-453.

Sasahara H., T. Obikawa and T. Shirakashi (2004) “Prediction model of surface residual stress within a machined surface by combining two orthogonal plane models.” Int. J. Machine Tools & Manufacture, 44, 815–822.

Thiele J.D and S.N. Melkote (2000). “Effect of tool edge geometry on workpiece subsurface deformation and through-thickness residual stresses for hard turning of aisi 52100 steel.” J. Manuf. Proc., 2, 270-276.

Warren A.W. and Y.B. Guo (2009). “Characteristics of residual stress profiles in hard turned versus ground surfaces with and without a white layer.” J. Manuf. Sci. Eng., 131/041004, 1-10.